




Candida auris Forms High-Burden Biofilms in Skin Niche Conditions and on Porcine Skin

Mark V. Horton,^{a,b} Chad J. Johnson,^a John F. Kernien,^a Tarika D. Patel,^a Brandon C. Lam,^a J. Z. Alex Cheong,^{a,b} Jennifer J. Meudt,^c Dhanansayan Shanmuganayagam,^c Lindsay R. Kalan,^{a,b}  Jeniel E. Nett^{a,b}

^aDepartment of Medicine, University of Wisconsin, Madison, Wisconsin, USA

^bDepartment of Medical Microbiology and Immunology, University of Wisconsin, Madison, Wisconsin, USA

^cDepartment of Animal Science, University of Wisconsin, Madison, Wisconsin, USA

ABSTRACT Emerging pathogen *Candida auris* causes nosocomial outbreaks of life-threatening invasive candidiasis. It is unclear how this species colonizes skin and spreads in health care facilities. Here, we analyzed *C. auris* growth in synthetic sweat medium designed to mimic axillary skin conditions. We show that *C. auris* demonstrates a high capacity for biofilm formation in this milieu, well beyond that observed for the most commonly isolated *Candida* sp., *Candida albicans*. The *C. auris* biofilms persist in environmental conditions expected in the hospital setting. To model *C. auris* skin colonization, we designed an *ex vivo* porcine skin model. We show that *C. auris* proliferates on porcine skin in multilayer biofilms. This capacity to thrive in skin niche conditions helps explain the propensity of *C. auris* to colonize skin, persist on medical devices, and rapidly spread in hospitals. These studies provide clinically relevant tools to further characterize this important growth modality.

IMPORTANCE The emerging fungal pathogen *Candida auris* causes invasive infections and is spreading in hospitals worldwide. Why this species exhibits the capacity to transfer efficiently among patients is unknown. Our findings reveal that *C. auris* forms high-burden biofilms in conditions mimicking sweat on the skin surface. These adherent biofilm communities persist in environmental conditions expected in the hospital setting. Using a pig skin model, we show that *C. auris* also forms high-burden biofilm structures on the skin surface. Identification of this mode of growth sheds light on how this recently described pathogen persists in hospital settings and spreads among patients.

KEYWORDS *Candida auris*, biofilm, pathogenicity, skin, porcine, sweat, transmission

For patients with invasive *Candida auris* infections, mortality rates can be exceedingly high, approaching 60% (1). Due to the severity of the infections and ongoing nosocomial outbreaks, *C. auris* has emerged as the first fungal pathogen to be designated a global public health threat (2). In the current report of antibiotic resistance threats in the United States, the Centers for Disease Control and Prevention lists *C. auris* as the highest-level threat. In health care settings, *C. auris* efficiently colonizes the skin, persists on hospital surfaces, and rapidly spreads among patients (1, 3, 4). As other *Candida* species typically colonize the gastrointestinal tract, the apparent propensity for *C. auris* to persist on the skin surface is a distinct trait, likely contributing to its efficient nosocomial transmission. However, despite the growing concern for *C. auris* infection within health care facilities, little is known regarding the mechanism of *C. auris* skin colonization.

Similarly to other *Candida* species, *C. auris* infections typically occur in patients with indwelling medical devices, such as vascular catheters, G tubes, and endotracheal tubes

Citation Horton MV, Johnson CJ, Kernien JF, Patel TD, Lam BC, Cheong JZA, Meudt JJ, Shanmuganayagam D, Kalan LR, Nett JE. 2020. *Candida auris* forms high-burden biofilms in skin niche conditions and on porcine skin. mSphere 5:e00910-19. <https://doi.org/10.1128/mSphere.00910-19>.

Editor Aaron P. Mitchell, University of Georgia

Copyright © 2020 Horton et al. This is an open-access article distributed under the terms of the [Creative Commons Attribution 4.0 International license](https://creativecommons.org/licenses/by/4.0/).

Address correspondence to Jeniel E. Nett, jenett@medicine.wisc.edu.

For a commentary on this article, see <https://doi.org/10.1128/mSphere.00972-19>.

Received 5 December 2019

Accepted 9 December 2019

Published 22 January 2020

(1, 5). On these artificial surfaces, *Candida* spp. produce biofilms, adherent microbial communities encased within a protective extracellular matrix (6, 7). While prior studies have demonstrated biofilm formation for *C. auris*, the observed structures are not nearly as dense as those formed by *Candida albicans*, the most prevalent *Candida* sp. (8–12). Due to the predilection of *C. auris* for skin, we questioned if *C. auris* may exhibit an enhanced capacity to proliferate in the cutaneous environment, whereby it could gain access to the bloodstream via the insertion and continued presence of vascular catheters. Here, we describe the remarkable ability of *C. auris* to form biofilms in conditions of the skin environment, mimicked experimentally using synthetic human sweat medium and an *ex vivo* porcine skin model.

RESULTS

C. auris forms high-burden biofilms in skin milieu. To assess the capacity of *C. auris* to proliferate in skin niche conditions, we produced synthetic sweat medium, designed to mimic human axillary sweat, and examined biofilm formation. After 24 h of incubation, *C. auris* produced dense biofilms with 10-fold greater burden than the biofilms formed by *C. albicans* (Fig. 1a) ($P < 0.05$). This is quite striking, as under typical laboratory conditions, *C. albicans* exhibits a capacity for biofilm formation well beyond that observed for most other *Candida* spp. (13). For example, in RPMI-MOPS (morpholinepropanesulfonic acid), the biomass of biofilms formed by *C. albicans* was 3-fold greater than for *C. auris* (Fig. 1a) ($P < 0.05$), consistent with prior studies demonstrating lower biofilm burdens for this species (8, 9).

To evaluate the biofilm architecture and cellular morphology of *C. auris* growing in skin niche conditions, we grew biofilms on coverslips and imaged them by scanning electron microscopy. Consistent with quantitative biofilm formation assays, *C. auris* growing in synthetic sweat medium replicated that on the coverslip surface, proliferating as a multilayer biofilm, composed entirely of yeast cells (Fig. 1b). In contrast, *C. albicans* formed a very rudimentary biofilm, composed of yeast with rare pseudohyphae or hyphae. Biofilm structures and burdens were vastly different for biofilms grown in RPMI-MOPS. In this tissue culture medium, *C. albicans* formed dense biofilms composed primarily of hyphae, while biofilms formed by *C. auris* appeared as a monolayer of yeast. These findings show that *C. auris* exhibits a heightened capacity to form biofilms in the milieu of the skin surface.

Circulating *C. auris* strains vary genetically and cluster into at least 4 distinct clades (1). The *C. auris* strain (B11203) selected for our initial experiments had been isolated from a patient in India and phylogenetically placed in the South Asian or India/Pakistan clade (1). Given the genetic diversity of strains, we questioned if the capacity for robust biofilm formation in skin niche conditions may represent a shared trait among *C. auris* strains. To address this question, we obtained a strain set from the Centers for Disease Control (see Table S1 in the supplemental material) which encompassed at least one isolate from each clade, and we examined biofilm formation (1). Biofilm growth by the majority of the strains paralleled that observed for *C. auris* B11203 (listed as strain 5), with burdens reaching approximately 10-fold that of *C. albicans* (see Fig. S1). We next considered if the differences in biofilm formation may be a consequence of general medium-specific growth differences. Indeed, the majority of *C. auris* strains appeared to have a slight growth advantage over *C. albicans* in the sweat medium under nonbiofilm conditions (see Fig. S2). However, these relatively small differences did not account for the 10-fold greater biofilm formation observed for *C. auris* (Fig. 1a and S1). The findings show that robust biofilm formation in skin niche conditions is a common characteristic for *C. auris*. As *C. auris* B11203 appeared representative of the *C. auris* isolates, we continued to utilize this strain for subsequent experiments.

C. auris biofilms formed in skin niche conditions resist desiccation. Next, we questioned if the formation of biofilm by *C. auris* in the skin milieu environment may serve as a mechanism to resist desiccation. We reasoned that desiccation might occur in two environments, either on the skin surface as sweat evaporates or in the environ-

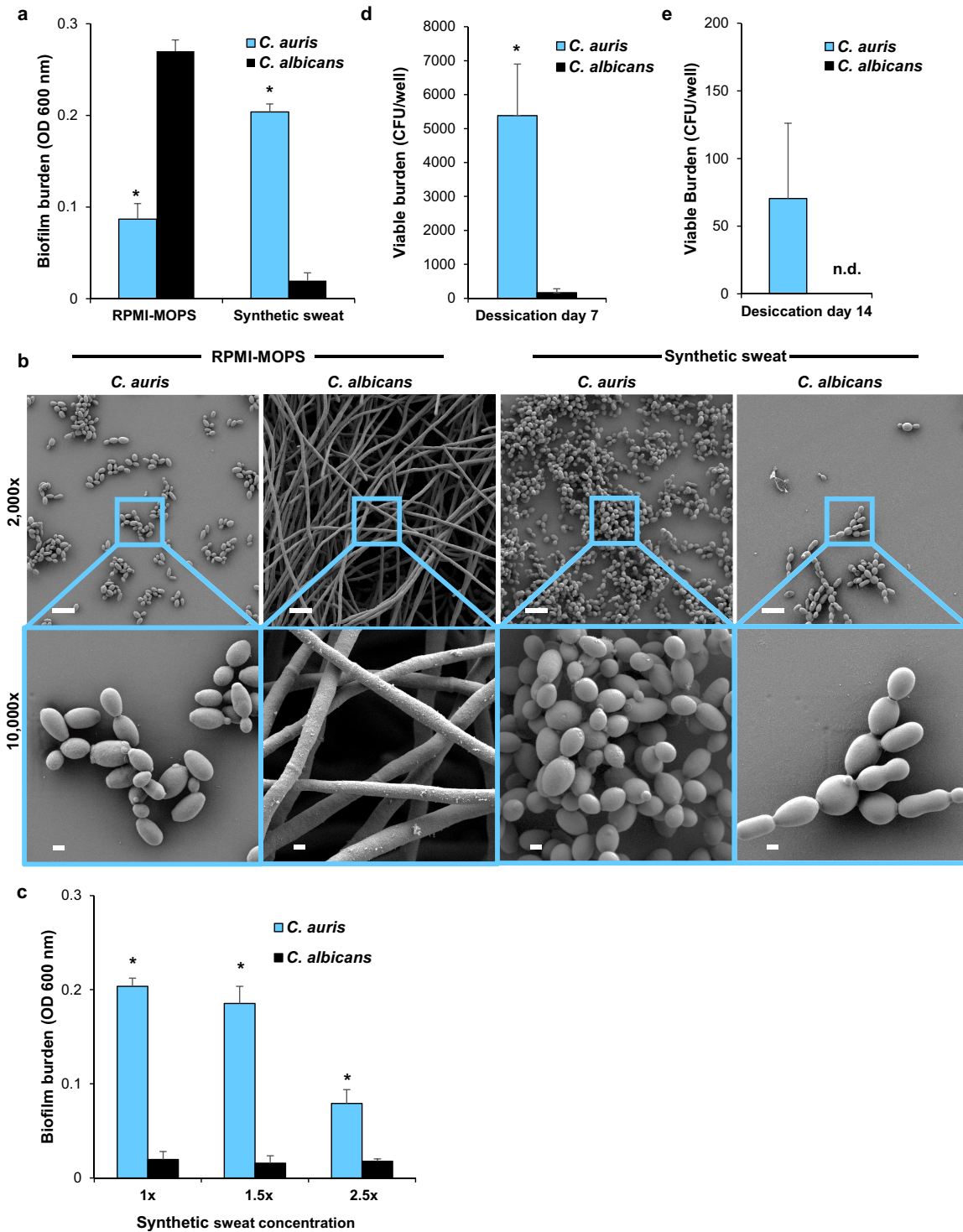


FIG 1 *C. auris* forms high-burden biofilms in synthetic sweat medium. (a) *Candida* biofilms were grown in RPMI-MOPS or synthetic sweat medium for 24 h, and biofilm burden was measured by absorbance at 600 nm. *C. auris* biofilm density was compared to that of *C. albicans* in each media by Student's *t* test, *, $P < 0.05$, standard errors of the means shown, $n = 3$. (b) *Candida* biofilms were grown on coverslips (24 h) and imaged with scanning electron microscopy. Bars, 10 μm and 1 μm for $\times 2,000$ and $\times 10,000$ magnification images, respectively. (c) *Candida* biofilms were grown in various concentrations of synthetic sweat medium for 24 h, *, $P < 0.05$ by Student's *t* test at each concentration, standard errors of the means shown, $n = 3$. (d and e) *Candida* biofilms were subjected to 24 h of desiccation, and viable burdens were assessed by plating of serial dilutions of disrupted biofilms after 7 or 14 days, *, $P < 0.05$ by Student's *t* test, standard errors of the means shown, $n = 6$; n.d., not detected.

ment where sweat and desquamated skin dry on surfaces. As sweat evaporates, the concentration of salt and other components increases. To mimic this process on the skin surface, we concentrated synthetic sweat medium and examined the influence on biofilm formation. In 1.5 \times -concentrated synthetic sweat, *C. auris* formed high-burden biofilms, 10-fold greater than *C. albicans*, mirroring the findings observed for the nonconcentrated sweat (Fig. 1c). Even in 2.5 \times -concentrated sweat, *C. auris* exhibited the capacity to proliferate as a biofilm. The burdens of these biofilms were below those formed in the less-concentrated sweat but were still 4-fold greater than the biofilms formed by *C. albicans*.

To model environmental drying of sweat and desquamated skin, we produced biofilms in synthetic sweat medium and subjected the biofilms to 24 h of desiccation in a laminar flow hood. At 7 days postdesiccation, we found *C. auris* to persist at a burden approximately 30-fold greater than *C. albicans* (Fig. 1d). At 14 days postdesiccation, *C. auris* grew readily from biofilms, while *C. albicans* biofilms were not viable (Fig. 1e). Taken together, these results illustrate that biofilms formed by *C. auris* in conditions of the skin microenvironment persist despite conditions of both sweat evaporation and environmental desiccation.

***C. auris* forms high-burden biofilms in skin niche conditions on porcine skin.** To simulate *C. auris* growth in the skin niche, we developed an *ex vivo* porcine skin model employing the Wisconsin Miniature Swine (14). Pig skin was selected based on the many characteristics it shares with human skin, including similarities in the thickness of skin layers, the types and distribution of skin cells, and the mechanisms of skin repair (15–18). As conventional pigs have been bred for increased size and muscle mass, miniature varieties more closely mimic human body composition (14, 15). Full-thickness skin samples were harvested from excised skin and placed in semisolid medium to supply nutrients to the dermis (Fig. 2a). The addition of paraffin to the medium-epidermal interface provided a barrier between the dermal medium and the skin surface, allowing these compartments to remain separated and limiting *Candida* growth to the skin surface. Following inoculation of the epidermis with *Candida* suspended in synthetic sweat medium, we allowed the samples to incubate for 24 h, at which time the sweat medium had evaporated. Consistent with our *in vitro* observations, *C. auris* exhibited enhanced growth compared to that of *C. albicans* in this environment, with *C. auris* propagating to a burden nearly 15-fold greater than *C. albicans* and replicating nearly 100-fold above the initial inoculum (Fig. 2b) ($P < 0.05$).

We next utilized scanning electron microscopy to assess the distribution of *C. auris* biomass, the architecture of skin-associated biofilms, and the interaction of *Candida* with the epidermal surface. Following inoculation of *C. auris*, imaging of the porcine skin at low magnification revealed diffuse fungal growth over the epidermal surface (Fig. 2c). Higher magnification imaging showed the formation of multilayer biofilms composed of yeast cells. In contrast, imaging of porcine skins inoculated with *C. albicans* showed little fungal growth. Multilayer aggregates were not observed. Examination of the fungal-epithelial interface for both species revealed intact skin without evidence of tissue invasion. This lack of invasion supports the use of porcine skin to model human skin colonization, as this process does not involve tissue destruction by fungi. Furthermore, the results reveal that *C. auris* exhibits an enhanced propensity to proliferate on porcine skin.

DISCUSSION

The results of these studies shed light on the capacity of *C. auris* to proliferate and persist on the skin surface and in environmental conditions involving skin components. Our findings demonstrate that growth in synthetic sweat medium and on porcine skin allows *C. auris* to form dense biofilms that flourish in conditions of evaporation and resist desiccation. These observations help to explain this pathogen's propensity for colonizing skin, persisting on hospital surfaces, and spreading efficiently in the hospital setting (4, 19). As an example, a *C. auris* outbreak in the United Kingdom was linked to the use of reusable axillary temperature probes (20). Given the axillary skin environ-

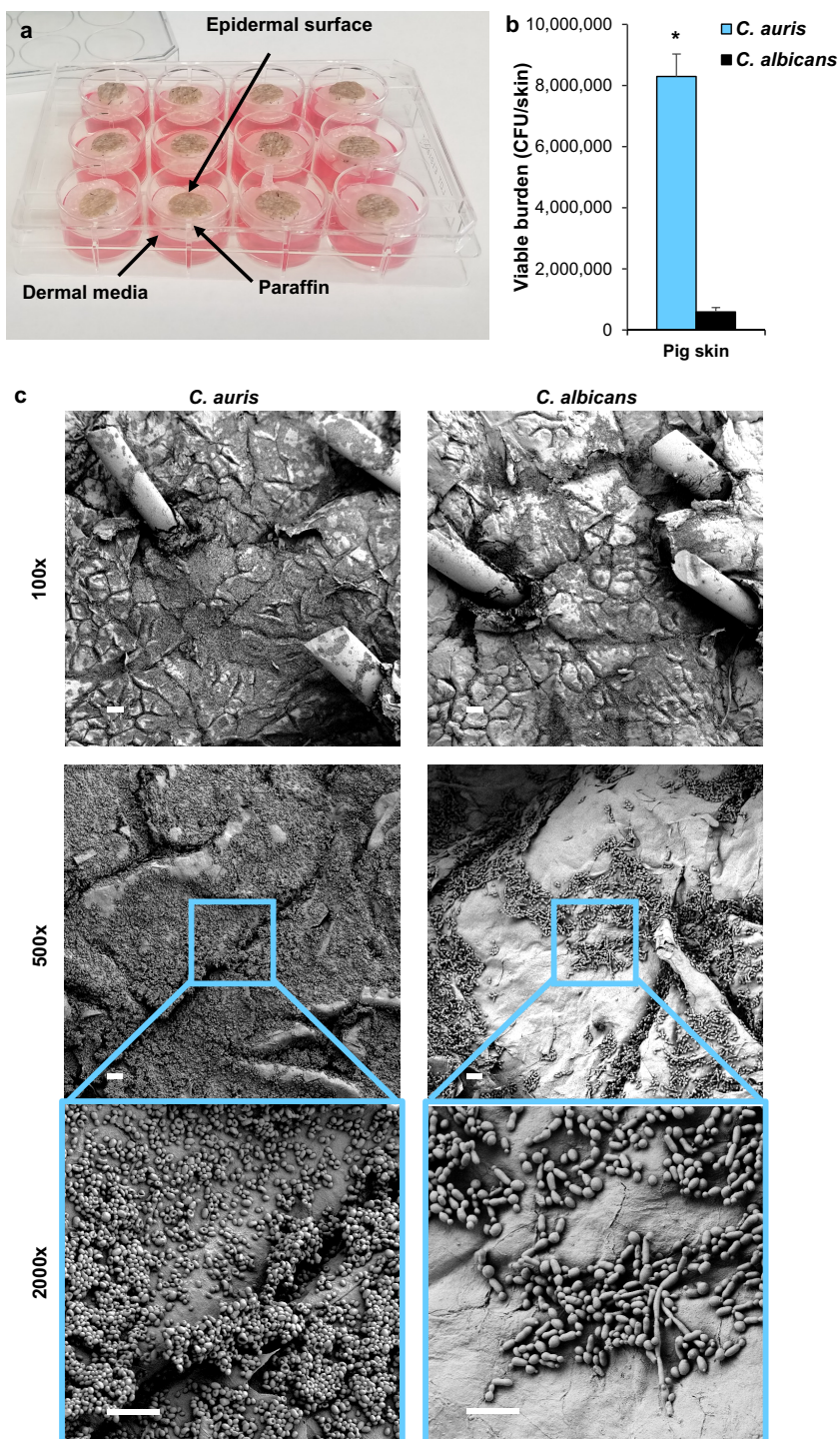


FIG 2 *C. auris* effectively colonizes porcine skin. (a) Porcine skin samples were placed in DMEM supplemented with 10% FBS and set in paraffin to separate the epidermal surface from the liquid medium. *Candida* cells suspended in synthetic sweat medium were inoculated on the epidermal surface. (b) *Candida* cultures were suspended in synthetic sweat medium inoculated on the surface of porcine skin samples. Following 24 h of incubation, *Candida* growth on the hair and skin surface was enumerated via CFU counts. *, $P < 0.05$ by Student's *t* test, standard errors of the means shown, $n = 4$. (c) *Candida* biofilms were grown on porcine skin samples and imaged with scanning electron microscopy. Bars, 100 μm , 20 μm , and 10 μm for $\times 100$, $\times 500$, and $\times 2,000$ magnification, respectively.

ment in this setting, we propose that the outbreak likely involved robust biofilm growth similar to that observed in the present study. We also postulate that other reusable equipment, such as blood pressure cuffs and intravenous infusion pumps, can harbor resilient *C. auris* biofilms. These items are also in frequent contact with skin and often shared among patients.

Our finding that *C. auris* resists desiccation during biofilm formation may not be surprising, as a prior study has shown this species to survive dry conditions for up to 2 weeks (21). Little is known about the mechanism(s) utilized by *C. auris* to resist desiccation. However, studies by Day and colleagues characterized the responses of *Candida* to a variety of stresses, including high salinity, and showed that *C. auris* exhibited a unique stress resistance profile compared to those of other *Candida* spp. (22). Despite the different profiles, these responses involved the evolutionarily conserved Hog1 stress-activated protein kinase (SAPK). It is intriguing to speculate that biofilm formation and resistance to desiccation may be intertwined with this pathway. In addition, the karyotypic plasticity displayed by *C. auris* in response to stressors may contribute to this organism's ability to adapt and persist in the skin niche (23). Further understanding of these stress tolerance pathways may lead to identifying new approaches to eradicate *C. auris* from the environment, to prevent person-to-person spread, or to pharmaceutically target *C. auris*.

What is striking about *C. auris* is that individual strains appear to have arisen independently in remote geographic locations (1). While an environmental niche for *C. auris* has not been described, one hypothesis is that increasing temperatures due to climate change promoted the emergence of this species that could then thrive in the high temperatures of mammalian and avian hosts (24). Because biofilm formation is a mechanism for adherence and persistence in various environments, insight into factors governing *C. auris* robust biofilms may also help elucidate environmental factors that have contributed to the emergence of this organism.

The present study provides tools to further dissect *C. auris* growth and biofilm formation in the skin environment. In light of the similarities to human skin, porcine skin serves as an excellent model for studies of wound healing, infection, and skin colonization (15–18, 25). Growth of *C. auris* in this *ex vivo* model mimics what is observed clinically, an enhanced capacity for skin colonization. Understanding the interactions of *C. auris* with skin and the pathways involved in biofilm formation may provide insight into new strategies to control the spread of this emerging pathogen.

MATERIALS AND METHODS

Organisms and inoculum. Studies included *C. albicans* SC5314 and *C. auris* strains provided by the Centers for Disease Control and Prevention (see Table S1 in the supplemental material) (1). Strains were maintained on yeast extract-peptone-dextrose (YPD) plates and propagated in YPD broth overnight in an orbital shaker at 30°C. Overnight cultures were diluted 1:1,000 in Dulbecco's phosphate-buffered saline (DPBS), vortexed thoroughly, counted with a hemocytometer, and adjusted to 10⁶ cells/ml in RPMI-MOPS or synthetic sweat medium.

Synthetic sweat medium. Artificial human axillary sweat medium was adapted from that described by Callewaert et al. (26) with several modifications (Table S2). In place of fatty acids hydrolyzed from human abdominal subcutaneous fat, we included a mix of the three most abundance fatty acids found in human sweat (lauric, myristic, and palmitic fatty acids) (26, 27). In light of this, lower concentrations of fatty acids were added to ensure solubility. Cholesterol and lactic acid concentrations were selected based on prior measurements for sweat (28, 29). Medium was made at a 2.5× concentration, warmed to 60°C with stirring, and filter sterilized. Medium was stored at room temperature and diluted to 1× concentration with sterile water.

Biofilm and planktonic growth. For biofilm assays, 200 μl was added to flat-bottom 96-well microtiter plates (30). Following a 24 h of incubation at 37°C, biofilms were rinsed gently with DPBS, and 200 μl of DPBS was applied. The biofilm burdens were then measured by optical density at 600 nm (OD₆₀₀) values obtained using a microplate reader (Synergy H1; Bio-Tek Instruments) (31). For planktonic growth curves, 200 μl was similarly seeded in flat-bottom 96-well microtiter plates. Plates were then placed in the microplate reader with shaking at 37°C, and OD₆₀₀ values were obtained.

Desiccation assay. Biofilms were grown in flat-bottom 96-well microtiter plates for 24 h, as described above. After removing the medium and nonadherent cells, plates were desiccated in a laminar flow hood with lids removed for 24 h and subsequently incubated at room temperature. After 7 or 14 days, biofilms were harvested, vortexed, and plated on YPD agar for determination of viable burden.

Porcine skin model. The collection of porcine skin samples was conducted under protocols approved by the University of Wisconsin—Madison Institutional Animal Care and Use Committee in accordance with published National Institutes of Health (NIH) and United States Department of Agriculture (USDA) guidelines. Skin from euthanized animals was excised, washed alternately with DPBS and 70% ethanol (ETOH) until clean, and then shaved. Using a biopsy punch, 12-mm full-thickness skin samples were extracted and placed into the wells of 12-well plates, each containing 3 ml Dulbecco's modified Eagle medium (DMEM) supplemented 10% fetal bovine serum (FBS) (10%), penicillin (1,000 U/ml), and streptomycin (1 mg/ml). Samples were incubated at 37°C with 5% CO₂ for 18 h with one change of medium after 6 h. Tissues were then rinsed in DPBS, dried thoroughly, and placed on semisolid medium (6:4 ratio of 1% agarose in DPBS and DMEM with 10% FBS). To construct a barrier to separate the subdural medium (DMEM) and epidermal surface, 800 μl paraffin wax was applied to the inner surface of the DMEM at the epidermal interface. *C. auris* suspended in synthetic sweat medium (10⁷ cells/ml) was applied to the skin surface (10 μl). Following 24 h of incubation without a humidity source at 37°C with 5% CO₂, skin samples were processed for scanning electron microscopy (described below) or vortexed in DPBS and plated for assessment of viable burden.

Scanning electron microscopy. *Candida* biofilms were examined by scanning electron microscopy as previously described (32, 33). Briefly, 13-mm Thermanox coverslips were coated with 4 μg/ml fibrinogen in DPBS for 1 h at 37°C, rinsed twice with water, and dried for 2 h. Cultures of *Candida* (40 μl at 1.5 × 10⁷ cells/ml cultures in RPMI-MOPS or synthetic sweat medium) were added for 30 min, and then nonadherent cells were removed. Following replacement of the medium, coverslips were incubated at 37°C for 24 h, washed, and fixed overnight (4% formaldehyde, 1% glutaraldehyde, in DPBS). Samples were next washed with DPBS, treated with 1% osmium tetroxide, and then washed with DPBS. Samples were dehydrated with multiple ethanol washes, subjected to critical point drying, mounted on aluminum stubs, sputter coated with platinum, and imaged with a scanning electron microscope (LEO 1530) at 3 kV. Pig skin samples were similarly processed and mounted on aluminum stubs with carbon paint, and silver paint was applied around the perimeter for improved conductivity.

SUPPLEMENTAL MATERIAL

Supplemental material is available online only.

FIG S1, PDF file, 0.1 MB.

FIG S2, PDF file, 0.1 MB.

TABLE S1, DOCX file, 0.1 MB.

TABLE S2, DOCX file, 0.1 MB.

ACKNOWLEDGMENTS

We thank Shawn Lockhart for *Candida* strains.

This work was supported by the National Institutes of Health (K08 AI108727) and the Burroughs Wellcome Fund (1012299).

REFERENCES

- Lockhart SR, Etienne KA, Vallabhaneni S, Farooqi J, Chowdhary A, Govender NP, Colombo AL, Calvo B, Cuomo CA, Desjardins CA, Berkow EL, Castanheira M, Magobo RE, Jabeen K, Asghar RJ, Meis JF, Jackson B, Chiller T, Litvintseva AP. 2017. Simultaneous emergence of multidrug-resistant *Candida auris* on 3 continents confirmed by whole-genome sequencing and epidemiological analyses. *Clin Infect Dis* 64:134–140. <https://doi.org/10.1093/cid/ciw691>.
- Lamoth F, Kontoyiannis DP. 2018. The *Candida auris* alert: facts and perspectives. *J Infect Dis* 217:516–520. <https://doi.org/10.1093/infdis/jix597>.
- Rudramurthy SM, Chakrabarti A, Paul RA, Sood P, Kaur H, Kapoor MR, Kindo AJ, Marak RSK, Arora A, Sardana R, Das S, Chhina D, Patel A, Xess I, Tarai B, Singh P, Ghosh A. 2017. *Candida auris* candidaemia in Indian ICUs: analysis of risk factors. *J Antimicrob Chemother* 72:1794–1801. <https://doi.org/10.1093/jac/dkx034>.
- Schelenz S, Hagen F, Rhodes JL, Abdolrasouli A, Chowdhary A, Hall A, Ryan L, Shackleton J, Trimlett R, Meis JF, Armstrong-James D, Fisher MC. 2016. First hospital outbreak of the globally emerging *Candida auris* in a European hospital. *Antimicrob Resist Infect Control* 5:35. <https://doi.org/10.1186/s13756-016-0132-5>.
- Adams E, Quinn M, Tsay S, Poirot E, Chaturvedi S, Southwick K, Greenko J, Fernandez R, Kallen A, Vallabhaneni S, Haley V, Hutton B, Blog D, Lutterloh E, Zucker H, *Candida auris* Investigation Workgroup. 2018. *Candida auris* in healthcare facilities, New York, USA, 2013–2017. *Emerg Infect Dis* 24:1816–1824. <https://doi.org/10.3201/eid2410.180649>.
- Donlan RM. 2001. Biofilm formation: a clinically relevant microbiological process. *Clin Infect Dis* 33:1387–1392. <https://doi.org/10.1086/322972>.
- Kojic EM, Darouiche RO. 2004. *Candida* infections of medical devices. *Clin Microbiol Rev* 17:255–267. <https://doi.org/10.1128/cmr.17.2.255-267.2004>.
- Larkin E, Hager C, Chandra J, Mukherjee PK, Retuerto M, Salem I, Long L, Isham N, Kovanda L, Borroto-Esoda K, Wring S, Angulo D, Ghannoum M. 2017. The emerging pathogen *Candida auris*: growth phenotype, virulence factors, activity of antifungals, and effect of SCY-078, a novel glucan synthesis inhibitor, on growth morphology and biofilm formation. *Antimicrob Agents Chemother* 61:e02396-16. <https://doi.org/10.1128/AAC.02396-16>.
- Sherry L, Ramage G, Kean R, Borman A, Johnson EM, Richardson MD, Rautemaa-Richardson R. 2017. Biofilm-forming capability of highly virulent, multidrug-resistant *Candida auris*. *Emerg Infect Dis* 23:328–331. <https://doi.org/10.3201/eid2302.161320>.
- Dominguez EG, Zarnowski R, Choy HL, Zhao M, Sanchez H, Nett JE, Andes DR. 2019. Conserved role for biofilm matrix polysaccharides in *Candida auris* drug resistance. *mSphere* 4:e00680-18. <https://doi.org/10.1128/mSphereDirect.00680-18>.
- Kean R, Delaney C, Sherry L, Borman A, Johnson EM, Richardson MD, Rautemaa-Richardson R, Williams C, Ramage G. 2018. Transcriptome assembly and profiling of *Candida auris* reveals novel insights into biofilm-mediated resistance. *mSphere* 3:e003340-18. <https://doi.org/10.1128/mSphere.00334-18>.
- Singh R, Kaur M, Chakrabarti A, Shankarnarayan SA, Rudramurthy SM. 2019. Biofilm formation by *Candida auris* isolated from colonising sites and candidemia cases. *Mycoses* 62:706–709. <https://doi.org/10.1111/myc.12947>.

13. Kuhn DM, Chandra J, Mukherjee PK, Ghannoum MA. 2002. Comparison of biofilms formed by *Candida albicans* and *Candida parapsilosis* on bioprosthetic surfaces. *Infect Immun* 70:878–888. <https://doi.org/10.1128/iai.70.2.878-888.2002>.
14. Schomberg DT, Tellez A, Meudt JJ, Brady DA, Dillon KN, Arowolo FK, Wicks J, Rousselle SD, Shanmuganayagam D. 2016. Miniature swine for preclinical modeling of complexities of human disease for translational scientific discovery and accelerated development of therapies and medical devices. *Toxicol Pathol* 44:299–314. <https://doi.org/10.1177/0192623315618292>.
15. Liu Y, Chen JY, Shang HT, Liu CE, Wang Y, Niu R, Wu J, Wei H. 2010. Light microscopic, electron microscopic, and immunohistochemical comparison of Bama minipig (*Sus scrofa domestica*) and human skin. *Comp Med* 60:142–148.
16. Eaglstein WH, Mertz PM. 1978. New methods for assessing epidermal wound healing: the effects of triamcinolone acetonide and polyethylene film occlusion. *J Invest Dermatol* 71:382–384. <https://doi.org/10.1111/1523-1747.ep12556814>.
17. Sullivan TP, Eaglstein WH, Davis SC, Mertz P. 2001. The pig as a model for human wound healing. *Wound Repair Regen* 9:66–76. <https://doi.org/10.1046/j.1524-475x.2001.00066.x>.
18. Summerfield A, Meurens F, Ricklin ME. 2015. The immunology of the porcine skin and its value as a model for human skin. *Mol Immunol* 66:14–21. <https://doi.org/10.1016/j.molimm.2014.10.023>.
19. Vallabhaneni S, Kallen A, Tsay S, Chow N, Welsh R, Kerins J, Kemble SK, Pacilli M, Black SR, Landon E, Ridgway J, Palmore TN, Zelzany A, Adams EH, Quinn M, Chaturvedi S, Greenko J, Fernandez R, Southwick K, Furuya EY, Calfee DP, Hamula C, Patel G, Barrett P, MSD, Lafaro P, Berkow EL, Moulton-Meissner H, Noble-Wang J, Fagan RP, Jackson BR, Lockhart SR, Litvintseva AP, Chiller TM. 2016. Investigation of the first seven reported cases of *Candida auris*, a globally emerging invasive, multidrug-resistant fungus - United States, May 2013-August 2016. *MMWR Morb Mortal Wkly Rep* 65:1234–1237. <https://doi.org/10.15585/mmwr.mm6544e1>.
20. Eyre DW, Sheppard AE, Madder H, Moir I, Moroney R, Quan TP, Griffiths D, George S, Butcher L, Morgan M, Newnham R, Sunderland M, Clarke T, Foster D, Hoffman P, Borman AM, Johnson EM, Moore G, Brown CS, Walker AS, Peto TEA, Crook DW, Jeffery KJM. 2018. A *Candida auris* outbreak and its control in an intensive care setting. *N Engl J Med* 379:1322–1331. <https://doi.org/10.1056/NEJMoa1714373>.
21. Welsh RM, Bentz ML, Shams A, Houston H, Lyons A, Rose LJ, Litvintseva AP. 2017. Survival, persistence, and isolation of the emerging multidrug-resistant pathogenic yeast *Candida auris* on a plastic health care surface. *J Clin Microbiol* 55:2996–3005. <https://doi.org/10.1128/JCM.00921-17>.
22. Day AM, McNiff MM, da Silva Dantas A, Gow NAR, Quinn J. 2018. Hog1 regulates stress tolerance and virulence in the emerging fungal pathogen *Candida auris*. *mSphere* 3:e00506-18. <https://doi.org/10.1128/mSphere.00506-18>.
23. Bravo Ruiz G, Ross ZK, Holmes E, Schelenz S, Gow NAR, Lorenz A. 2019. Rapid and extensive karyotype diversification in haploid clinical *Candida auris* isolates. *Curr Genet* 65:1217–1228. <https://doi.org/10.1007/s00294-019-00976-w>.
24. Casadevall A, Kontoyiannis DP, Robert V. 2019. On the emergence of *Candida auris*: climate change, azoles, swamps, and birds. *mBio* 10:e01397-19. <https://doi.org/10.1128/mBio.01397-19>.
25. Giotis ES, Loeffler A, Knight-Jones T, Lloyd DH. 2012. Development of a skin colonization model in gnotobiotic piglets for the study of the microbial ecology of methicillin-resistant *Staphylococcus aureus* ST398. *J Appl Microbiol* 113:992–1000. <https://doi.org/10.1111/j.1365-2672.2012.05397.x>.
26. Callewaert C, Buyschaert B, Vossen E, Fievez V, Van de Wiele T, Boon N. 2014. Artificial sweat composition to grow and sustain a mixed human axillary microbiome. *J Microbiol Methods* 103:6–8. <https://doi.org/10.1016/j.mimet.2014.05.005>.
27. Nunome Y, Tsuda T, Kitagawa K. 2010. Determination of fatty acids in human sweat during fasting using GC/MS. *Anal Sci* 26:917–919. <https://doi.org/10.2116/analsci.26.917>.
28. Takemura T, Wertz PW, Sato K. 1989. Free fatty acids and sterols in human eccrine sweat. *Br J Dermatol* 120:43–47. <https://doi.org/10.1111/j.1365-2133.1989.tb07764.x>.
29. Thurmon FM, Ottenstein B. 1952. Studie on the chemistry of human perspiration with especial reference to its lactic acid content. *J Invest Dermatol* 18:333–339. <https://doi.org/10.1038/jid.1952.38>.
30. Nett JE, Cain MT, Crawford K, Andes DR. 2011. Optimizing a *Candida* biofilm microtiter plate model for measurement of antifungal susceptibility by tetrazolium salt assay. *J Clin Microbiol* 49:1426–1433. <https://doi.org/10.1128/JCM.02273-10>.
31. Lohse MB, Gulati M, Valle Arevalo A, Fishburn A, Johnson AD, Nobile CJ. 2017. Assessment and optimizations of *Candida albicans* *in vitro* biofilm assays. *Antimicrob Agents Chemother* 61:e02749-16. <https://doi.org/10.1128/AAC.02749-16>.
32. Johnson CJ, Kernien JF, Hoyer AR, Nett JE. 2017. Mechanisms involved in the triggering of neutrophil extracellular traps (NETs) by *Candida glabrata* during planktonic and biofilm growth. *Sci Rep* 7:13065. <https://doi.org/10.1038/s41598-017-13588-6>.
33. Johnson CJ, Cabezas-Olcoz J, Kernien JF, Wang SX, Beebe DJ, Huttenlocher A, Ansari H, Nett JE. 2016. The extracellular matrix of *Candida albicans* biofilms impairs formation of neutrophil extracellular traps. *PLoS Pathog* 12:e1005884. <https://doi.org/10.1371/journal.ppat.1005884>.